Probing the spin and orbital high-field susceptibility of magnetic solids on the basis of the XMCD sum rules

2009 J. Phys.: Condens. Matter 21 326004

(http://iopscience.iop.org/0953-8984/21/32/326004)

J. Phys.: Condens. Matter **21** (2009) 326004 (6pp) doi:10.1088/0953-8984/21/32/326004

Probing the spin and orbital high-field susceptibility of magnetic solids on the basis of the XMCD sum rules

H Ebert and S Mankovsky

Department Chemie und Biochemie/Physikalische Chemie, Universität München, Butenandtstraße 5-13, D-81377 München, Germany

Received 24 April 2009, in final form 18 June 2009
Published 20 July 2009
Online at stacks.iop.org/JPhysCM/21/326004

Abstract

It is demonstrated that the magnetic circular dichroism in x-ray absorption (XMCD) can be used to probe the spin and orbital high-field susceptibilities of spontaneously magnetic solids on the basis of the so-called XMCD sum rules. A corresponding theoretical description is presented that is formulated in terms of the fully relativistic multiple scattering Green's function formalism. Examples for the field-induced changes in XMCD spectra are given together with an application of the sum rules to these spectra that demonstrates their relation to the high-field susceptibility.

(Some figures in this article are in colour only in the electronic version)

1. Introduction

The circular magnetic dichroism in x-ray absorption (XMCD) is now a widely used phenomenon to investigate the magnetic properties of spontaneously magnetized materials in a component-resolved way [1]. Most of the corresponding experimental investigations aim to deduce the element-specific spin and orbital magnetic moments on the basis of the so-called XMCD sum rules [1–4]. These allow us to relate the moments to linear combinations of energy integrals over XMCD spectra defined as the difference in absorption spectra for left and right circularly polarized x-rays. As an XMCD experiment probes the projection of a magnetic moment onto the direction of the incoming x-ray beam it is straightforwardly possible to follow the response of the magnetization to an external field. In particular this allows us to record hysteresis loops in an element-specific way and, for example, to study the interlayer coupling in layered magnetic systems in a most detailed way [5].

Another interesting application is the investigation of the magnetic anisotropy energy $\Delta E_{\rm aniso}(\hat{n}, \hat{n}')$ [6, 7]. This is based on the one hand on the access to the orbital moment $\mu_{\rm orb}$ and its anisotropy $\Delta\mu_{\rm orb}(\hat{n}, \hat{n}')$ via the XMCD, and on the other hand on the relation between $\Delta\mu_{\rm orb}$ and the anisotropy energy [8, 9]. Obviously, this type of experiment again has to be performed in the presence of an external field $B_{\rm ext}$ that is used to orient the magnetization along the orientations $\hat{n}(\hat{n}')$ which the energy difference $\Delta E_{\rm aniso}(\hat{n}, \hat{n}')$ refers to.

The last two applications deal with the response of a system to a static magnetic field. However, there are also a number of interesting XMCD experiments that exploit a time-dependent field. One example is the investigation of the relaxation after a strong magnetic field pulse [10]. While the first of this type of experiment used very small magnetic fields up to 30 mT the use of pulsed fields up to 35 T became possible during the last few years [11]. Such high fields obviously mean a pronounced perturbation to the ground state leading to metastable magnetic states or inducing an appreciable magnetization in otherwise non-magnetic solids. In fact, moderately high static magnetic fields up to about 5 T have been used a few years ago to study the induced magnetism via the XMCD [12]. In this contribution it is argued that high magnetic fields applied to spontaneously magnetized solids not only lead to an alignment of the domains in the sample and a subsequent saturation of the magnetization but in general to an additional induced magnetization that can be probed by the XMCD. In the following we give a description of this phenomenon that is based on *ab initio* electronic structure calculations. Corresponding applications to ferromagnetic transition-metal systems are meant to demonstrate the field-induced XMCD in these systems and the use of the XMCD sum rules to deduce their high-field susceptibility.

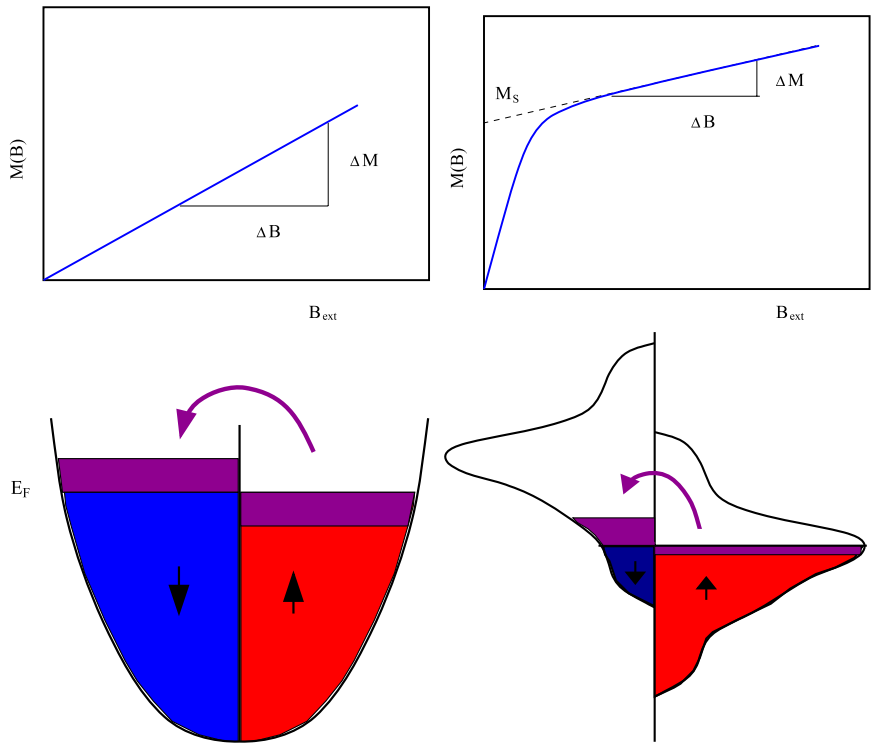

Figure 1. Dependence of the spin magnetization of a non-magnetic (left) and spontaneously ferromagnetic (right) solid on an external magnetic field. The lower panel shows the re-population of the electronic states due to a magnetic field leading to the spin susceptibility.

2. Theoretical framework

2.1. Basic considerations

For weak external fields $\vec{B}$ the magnetization $\vec{M}(\vec{B})$ induced in a non-magnetic solid will, in general, depend linearly on the field strength B as it is sketched in figure 1. Assuming a metallic system the induced magnetic moment is connected generally with a re-population of the states for spin up and down (see left column of figure 1). Linear response theory provides an adequate basis for this situation leading, for example, to the Pauli spin susceptibility $\chi_{\rm p}^0$ to be proportional to the density of states at the Fermi energy if the Stoner enhancement is ignored:

$$\chi_{\rm p}^0 = 2\mu_{\rm B}^2 n(E_{\rm F}) \tag{1}$$

with $\mu_{\rm B}$ being the Bohr magneton (see bottom left in figure 1).

In practice, however, the Stoner enhancement cannot be ignored and orbital $\chi_{\rm orb}$ contributions to the susceptibility of the same order as the spin susceptibility $\chi_{\rm spin}$ may contribute. In addition spin–orbit coupling may give rise to additional contributions to $\chi_{\rm spin}$ as well as $\chi_{\rm orb}$ [13]. A closed description of all these terms was worked out by the authors [14, 15] making use of a fully relativistic approach that expresses the response functions in terms of the Green's function that in turn is evaluated by means of multiple scattering theory or the Korringa–Kohn–Rostoker (KKR) band structure method. This formal basis was also used in the past to derive a parameter-free description of the XMCD on exactly the same footing. Accordingly, a combination of both the description for the magnetic susceptibility as well as for the XMCD could be done straightforwardly to arrive at a description of the field-induced XMCD in non-magnetic solids [16].

For a ferromagnet a weak external field will affect the domain structure and will lead to a single domain if it is strong enough. The apparently saturated magnetization will in general increase linearly with increasing field, as it is sketched in the right column of figure 1, with the slope of the magnetization curve $M(B)$ being the high-field susceptibility. Considering a metallic ferromagnet the corresponding unenhanced Pauli spin susceptibility $\chi_{\rm p}^0$ is given by [17]

$$\chi_{\rm p}^0 = 4\mu_{\rm B}^2 \left(\frac{1}{n^{\uparrow}(E_{\rm F})} + \frac{1}{n^{\downarrow}(E_{\rm F})} \right)^{-1}, \tag{2}$$

where $n^{\uparrow(\downarrow)}(E_{\rm F})$ are the spin-resolved densities of states at the Fermi level (see bottom right in figure 1).

As could be demonstrated by the authors, the above-mentioned linear response formalism allows us also to deal with systems with a spontaneous magnetization present in the ground state. This gave access among others to all spin and orbital contributions to the high-field susceptibility including all influences due to the presence of spin–orbit coupling [18]. Accordingly, it is quite natural to also apply the combined description of induced magnetization and XMCD mentioned above to spontaneously magnetized solids. As there are only a few practical differences for these two situations only the major features are given in the following.

2.2. Combined description of induced magnetization and field-induced XMCD in magnetic solids

The Green's function formalism allows us to describe the influence of an external magnetic field in a very elegant way by means of the so-called Dyson equation. Representing the field-free case by the Green's function G^0, the Green's function G^B for the finite field case is given by (in operator form, with the energy dependency suppressed)

$$G^B = G^0 + G^0 \Delta\mathcal{H}_B G^B. \tag{3}$$

Here $\Delta\mathcal{H}_B$ represents the perturbation of the system due to the field that stems from the direct Zeeman-type coupling of the spin and orbital degrees of freedom to the external field $B_{\rm ext}$ as well as a feedback term due to changes of the electron–electron interaction:

$$\Delta\mathcal{H}_B(\vec{r}) = \underbrace{\beta\sigma_z\mu_{\rm B}B_{\rm ext} + \beta\hat{l}_z\mu_{\rm B}B_{\rm ext}}_{\text{Zeeman}} + \underbrace{\Delta v^{\rm xc}(\vec{r}) + \Delta v^{\mathcal{H}}(\vec{r})}_{\text{Stoner}}. \tag{4}$$

The latter term gives rise to Stoner-type enhancement effects and may be treated within spin density functional theory, i.e. in practice by the local spin density approximation (LSDA) [19–21]. It should be emphasized that, in contrast to non-magnetic solids, this term will in general include contributions to charge rearrangements or charge transfer as well as a change $\Delta E_{\rm F}$ in the Fermi energy (for more details see [18]).

Applying a first-order approximation to equation (3), i.e. restricting to linear response, G_B is given by

$$G^B = G^0 + G^0\Delta\mathcal{H}_B G^0 = G^0 + \delta G^B, \tag{5}$$

where δG^B represents the distortion of the electronic system and allows us to express all field-induced properties. Assuming a collinear magnetization oriented along $\hat{z}$ the spin magnetization $\Delta m_{\rm spin}(\vec{r})$ may be written as

$$\Delta m_{\rm spin}(r) = -\frac{\mu_{\rm B}}{\pi}\Delta E_{\rm F}\,{\rm Im\,Trace}\beta\sigma_z G_0(E_{\rm F}) - \frac{\mu_{\rm B}}{\pi}{\rm Trace\,Im}\int^{E_{\rm F}} {\rm d}E\,\beta\sigma_z G_0\Delta\mathcal{H}_B G_0 \tag{6}$$

with corresponding expressions for the induced orbital magnetization $\Delta m_{\rm orb}(\vec{r})$ and charge density $\Delta n(\vec{r})$. Here it should be noted that the perturbation $\Delta\mathcal{H}_B$ implicitly depends on the induced densities $\Delta m_{\rm spin}(\vec{r})$, $\Delta m_{\rm orb}(\vec{r})$ and $\Delta n(\vec{r})$ as well as the Fermi energy shift $\Delta E_{\rm F}$. As a consequence the equations for these quantities have to be solved simultaneously also fixing δG^B this way.

With the influence of the external field expressed by equation (5), the corresponding x-ray absorption coefficient can be calculated from the standard expression [22–24]

$$\mu_\lambda^B(\omega) \propto \sum_i \langle\Phi_i|X_{\vec{q}\lambda}^\dagger G^B(E)X_{\vec{q}\lambda}|\Phi_i\rangle\,\Theta(E-E_{\rm F}). \tag{7}$$

Here the wavefunction Φ_i represents the various core states i involved in transitions due to a radiation field with frequency ω, wavevector $\vec{q}$ and polarization λ represented by the operator $X_{\vec{q}\lambda}$ (for more details see [23]). The final states above the Fermi energy $E_{\rm F}$ are represented by the Green's function G^B. According to the splitting of G^B into $G^0 + \delta G^B$ in equation (5) one has two corresponding contributions to the absorption coefficient:

$$\mu_\lambda^B(\omega) = \mu_\lambda^0(\omega) + \delta\mu_\lambda^B(\omega). \tag{8}$$

Obviously, the first term connected with G^0 is the one usually considered for a magnetic solid. This means the corresponding circular dichroic signal:

$$\Delta\mu^0 = \mu_+^0 - \mu_-^0 \tag{9}$$

is connected to the ground state magnetization. The second term, on the other hand, represents the field-induced change in absorption with

$$\delta\mu^B = \delta\mu_+^B - \delta\mu_-^B \tag{10}$$

giving the circular dichroism connected with the induced magnetization. As the latter one is treated in linear order, $\delta\mu^B$ will also be proportional to the external field.

As mentioned above the XMCD sum rules provide a linear relation between the XMCD signal $\Delta\mu$ and the spin and orbital moments, $\mu_{\rm spin}$ and $\mu_{\rm orb}$, respectively, of the absorbing atom. These relations have been derived originally starting from an atomic-like non-relativistic description of the electronic structure including spin–orbit coupling as a correction to this [1–4]. The additional various simplifying assumptions used to derive the XMCD sum rules have been listed, for example, in [25]. From this it is obvious that they are not applicable to all situations but may fail in special cases [26]. In particular, the applicability to itinerant-electron magnets was questioned [27, 28]. However, alternative derivations for the XMCD sum rules [29, 30] together with numerous numerical studies [31–37, 23] demonstrated that their application to metallic ferromagnets should in general lead to deviations of not more than 5–10% between the calculated moments and the ones deduced from the calculated XMCD spectra using the sum rules.

As the XMCD spectra reflect the spin and orbital polarization of the electronic states including effects of an external magnetic field B, the sum rules give access to the spin and orbital moments ($\mu_{\rm spin(orb)}^B$) of the system perturbed by the presence of B. In the linear response regime $\mu_{\rm spin(orb)}^B$ can be split into its part $\mu_{\rm spin(orb)}^0$ connected with the unperturbed ground state and its field-induced contribution $\Delta\mu_{\rm spin(orb)}$. The latter one varies linearly with B, i.e. one has $\Delta\mu_{\rm spin(orb)} = \chi_{\rm spin(orb)}\dot{B}$, with $\chi_{\rm spin(orb)}$ the corresponding spin (orbital) high-field susceptibility. The one-to-one correspondence of the XMCD spectrum $\Delta\mu^0$ and the moments $\mu_{\rm spin(orb)}^0$ for the unperturbed case on the one hand and the XMCD spectrum $\delta\mu^B$ and the moments $\Delta\mu_{\rm spin(orb)}$ on the other hand allow us to separate the ground state from the induced properties due to their different field dependence. As $\delta\mu_\lambda^B$ as well as the connected induced moments $\Delta\mu_{\rm spin(orb)}$ are proportional to B, division of the corresponding sum rules for the induced quantities by B leads for $L_{2,3}$ absorption edges to

$$\frac{1}{B}\int\left(\delta\mu_{L_3}^B - 2\delta\mu_{L_2}^B\right){\rm d}E = \frac{N}{3N_h\mu_{\rm B}}\left(\chi_{\rm spin} + 7\chi_T\right), \tag{11}$$

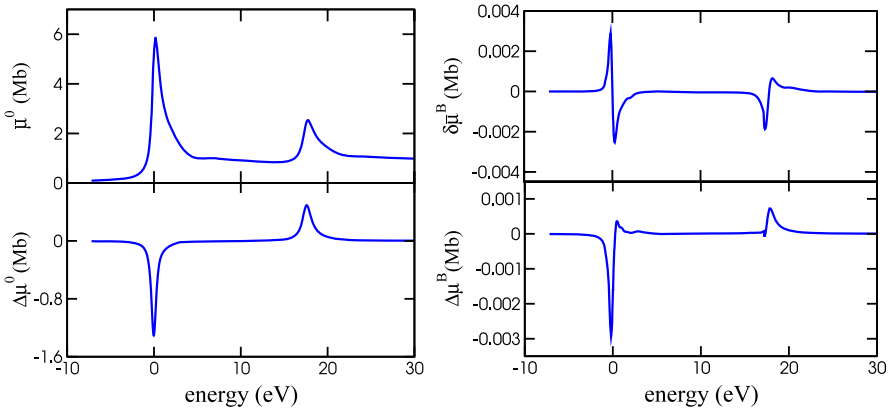

Figure 2. The left column shows the calculated x-ray absorption spectra $\bar{\mu}^0$ (top) for the $L_{2,3}$ edges of Ni together with the corresponding magnetic XMCD spectrum $\Delta\mu^0$ (bottom) for the ground state, i.e. no external field present. The right column shows the corresponding field-induced changes $\delta\bar{\mu}^B$ and $\Delta\mu^B$, respectively, for an external field of 10 T.

$$\frac{1}{B}\int \left(\delta\mu^B_{L_3} + \delta\mu^B_{L_2}\right) \mathrm{d}E = \frac{N}{2N_h\mu_\mathrm{B}}\chi_\mathrm{orb}, \tag{12}$$

where the field-induced contribution to the spin-dipole moment connected with the spin-dipole operator T_z [4] is accounted for by a corresponding high-field susceptibility χ_T. Using linear response theory the high-field spin and orbital susceptibilities χ_spin and χ_orb can be calculated from the expressions

$$\chi_\mathrm{spin} = -\frac{\mu_\mathrm{B}}{\pi}\frac{P^\mathrm{s}_n(E_\mathrm{F})}{n(E_\mathrm{F})}\mathrm{Trace\ Im}\int^{E_\mathrm{F}} \mathrm{d}E\, G\Delta\bar{\mathcal{H}}G - \frac{\mu_\mathrm{B}}{\pi}\mathrm{Trace\ Im}\int^{E_\mathrm{F}} \mathrm{d}E\, \beta\sigma_z G_n\Delta\bar{\mathcal{H}}G_n, \tag{13}$$

$$\chi_\mathrm{orb} = -\frac{\mu_\mathrm{B}}{\pi}\frac{P^\mathrm{o}_n(E_\mathrm{F})}{n(E_\mathrm{F})}\mathrm{Trace\ Im}\int^{E_\mathrm{F}} \mathrm{d}E\, G\Delta\bar{\mathcal{H}}G - \frac{\mu_\mathrm{B}}{\pi}\mathrm{Trace\ Im}\int^{E_\mathrm{F}} \mathrm{d}E\, \beta l_z G_n\Delta\bar{\mathcal{H}}G_n, \tag{14}$$

where $n(E_\mathrm{F})$, $P^\mathrm{s}_n(E_\mathrm{F})$ and $P^\mathrm{o}_n(E_\mathrm{F})$ are the density of states, spin polarization and orbital polarization, respectively, at the Fermi energy E_F and $\Delta\bar{\mathcal{H}}$ is the distortion given by equation (4) divided by the field strength B (for more details see [18]). For χ_T a corresponding expression can be given [38].

Within a non-relativistic description χ^spin consists only of the Stoner-enhanced Pauli susceptibility χ_Pauli, while a fully relativistic treatment gives rise to a spin–orbit-induced cross-term χ_so due to the coupling of the field to the orbital degree of freedom:

$$\chi_\mathrm{spin} = \chi_\mathrm{Pauli} + \chi_\mathrm{so}. \tag{15}$$

Analogously, the Van Vleck term χ_VV would be the primary term to be considered in the context of the sum rules. Again, spin–orbit coupling gives rise to a cross-term χ_os due to the coupling of the field to the spin degree of freedom:

$$\chi_\mathrm{orb} = \chi_\mathrm{VV} + \chi_\mathrm{os}. \tag{16}$$

Finally, the susceptibility χ_T in equation (11) represents the induced dipolar magnetic moment connected with the T_z operator [39, 38].

3. Results and discussion

The scheme outlined above has been implemented using the fully relativistic spin-polarized KKR band structure method to calculate the electronic Green's function G^0 for magnetic solids [40]. Corresponding results for the high-field susceptibility χ of ferromagnetic transition metals and alloys, obtained on the basis of the LSDA, have been presented in a previous publication [18], where technical details concerning the implementation can be found. In the following we present and discuss results for the field-induced XMCD and its relation to the high-field susceptibility. To demonstrate the impact of an external field on the XAS and XMCD spectra corresponding results for the $L_{2,3}$ edges of ferromagnetic Ni are shown in figure 2. The panel at the bottom of figure 2 gives the corresponding changes of the spectra $\delta\bar{\mu}^B$ and $\Delta\mu^B$, respectively, induced by a field of 10 T. As one notes, even the polarization-averaged XAS spectrum $\bar{\mu}$ is modified in a noticeable way due to the resonance-like shape of the $\delta\bar{\mu}^B$ spectra. The corrections of the XMCD spectrum $\Delta\mu$ are expected to be comparable as for $\bar{\mu}$. For a field of 10 T the peak height for the $\Delta\mu$ spectrum should be changed by several tenths of a per cent and for that reason should be detectable. The shape of the corrections $\delta\mu^B$ to $\Delta\mu$ are obviously quite different from $\delta\bar{\mu}^B$ giving the change for $\bar{\mu}$. Comparing the sign and lineshape of the $\delta\mu^B$ spectrum with that of the $\Delta\mu^0$ spectrum positive values for the induced spin and orbital magnetic moments may be expected on the basis of the XMCD sum rules presented in equations (11) and (12).

To test the applicability and reliability of the sum rules for a determination of the high-field susceptibility corresponding investigations were done for the ferromagnetic disordered alloy system Fe_xPt_{1-x}. Figure 3 shows results specific for Fe as a function of the concentration x. The open symbols present the bare and enhanced spin susceptibilities $\chi^{0\mathrm{Fe}}_\mathrm{spin}$ and $\chi^\mathrm{Fe}_\mathrm{spin}$, respectively, as well as the orbital Van Vleck susceptibility $\chi^\mathrm{Fe}_\mathrm{VV}$ of Fe as calculated directly using the response formalism (see equations (13) and (14)). As one notes the Stoner enhancement of $\chi^{0\mathrm{Fe}}_\mathrm{spin}$ is smaller than a factor of 2. The resulting enhanced susceptibility $\chi^\mathrm{Fe}_\mathrm{spin}$ is less than 50% of the orbital Van Vleck

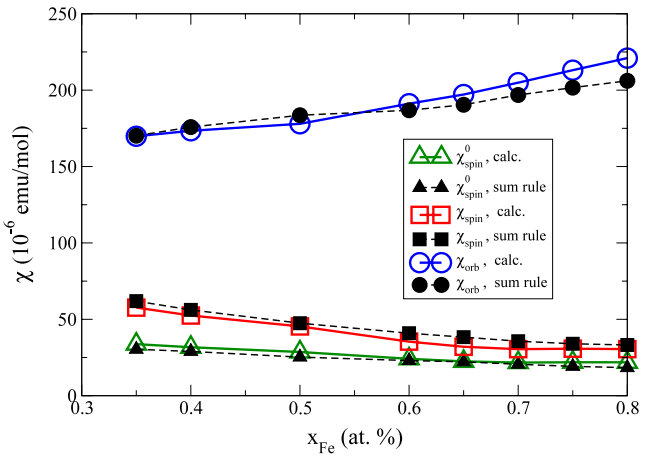

Figure 3. Spin and orbital high-field susceptibilities calculated directly via equations (13) and (14) (open symbols) for Fe in the disordered alloy Fe_xPt_{1-x} as a function of the concentration. In addition results for the susceptibilities are shown have been deduced from calculated $L_{2,3}$ XMCD spectra of Fe using the sum rules in equations (11) and (12).

susceptibility χ_{VV}^{Fe} for all concentrations. This situation is similar to the ferromagnetic alloy system Fe_xCo_{1-x}, where the Van Vleck susceptibility exceeds the spin susceptibility χ_{spin}^{Fe} by more than a factor of 3 for all concentrations. Also for Fe_xCo_{1-x} χ_{orb}^{Fe} varies only weakly with concentration, while χ_{spin}^{Fe} shows a rather pronounced concentration dependence with a maximum at about 90 at.% Fe content.

Figure 3 shows, in addition to the directly calculated susceptibilities, corresponding results deduced from the calculated $\Delta\mu^B$ spectra using the XMCD sum rules shown in equations (11) and (12). As one can see, the various spectroscopically deduced susceptibilities χ_{spin}^{0Fe}, χ_{spin}^{Fe} and χ_{VV}^{Fe} compare very well with their directly calculated counterparts. This holds concerning their relative magnitude as well as their variation with composition. Of course, no perfect matching of the corresponding directly calculated and spectroscopic susceptibility can be expected due to the various simplifying assumptions made in deriving the sum rules (see above). In applying the sum rules fixing the boundary for the integrals over the photon energies on the left-hand side of equations (11) and (12) introduce another uncertainty, as was extensively discussed in the literature (e.g. [31]). Finally, it has to be noted that for the comparison in figure 3 we neglected the contribution to the spectroscopic susceptibility χ_T due to the T_z term (see equation (11)). For the case of the field-induced XMCD in non-magnetic materials this was demonstrated to be well justified for cubic systems [38]. This should also hold here, as χ_T for Fe in fcc-Fe_xPt_{1-x} should be caused primarily by the relatively weak spin–orbit coupling of Fe.

The good agreement of the directly calculated susceptibilities with their counterparts obtained on the basis of the XMCD sum rules shown in figure 3 clearly demonstrates the applicability of the sum rules to the metallic ferromagnetic systems considered here. This implies that performing field-dependent XMCD measurements should indeed give a very reliable access to the component-specific high-field susceptibility that cannot be achieved so far by other means.

4. Summary

By comparing the situation for non-magnetic solids exposed to an external magnetic field arguments have been given that the XMCD should allow us to probe magnetic moments in magnetically ordered systems induced by high magnetic fields. Extending an approach recently developed by the authors for non-magnetic solids, a detailed theoretical description of the effect could be given. In particular the connection between the field-induced XMCD and the high-field susceptibility of the absorber atom was pointed out. Corresponding numerical studies performed with the spin-polarized relativistic KKR formalism in the framework of LSDA revealed the size of the expected field-induced XMCD, showing that it should be detectable. Furthermore it could clearly be demonstrated that there is a one-to-one correspondence of the susceptibilities calculated directly and those deduced from XMCD spectra. This clearly showed that the field-induced XMCD is indeed a suitable means to probe the spin and orbital contributions to the high-field susceptibility in a component-resolved way.

References

[1] Schütz G, Knülle M and Ebert H 1993 Magnetic circular x-ray dichroism and its relation to local moments *Phys. Scr.* T **49** 302

[2] Wienke R, Schütz G and Ebert H 1991 Determination of local magnetic moments of 5d-impurities in iron detected via spin-dependent absorption *J. Appl. Phys.* **69** 6147

[3] Thole B T, Carra P, Sette F and van der Laan G 1992 X-ray circular dichroism as a probe of orbital magnetization *Phys. Rev. Lett.* **68** 1943

[4] Carra P, Thole B T, Altarelli M and Wang X 1993 X-ray circular dichroism and local magnetic fields *Phys. Rev. Lett.* **70** 694

[5] Maccherozzi F, Sperl M, Minár G P J, Polesya S, Ebert H, Hochstrasser M, Rossi G, Wurstbauer U, Woltersdorf G, Wegscheider W and Back C H 2009 Evidence for magnetic proximity effect up to room temperature at Fe/(Ga, Mn) As interfaces *Phys. Rev. Lett.* **101** 267201

[6] Guo G Y, Ebert H, Temmerman W M and Durham P J 1994 Magnetic x-ray dichroism and anisotropy energy of Fe and Co multilayers *Metallic Alloys: Experimental and Theoretical Perspectives* ed J S Faulkner and R G Jordan (Dordrecht: Kluwer Academic)

[7] Grange W, Kappler J P, Maret M, Vogel J, Fontaine A, Petroff F, Krill G, Rogalev A, Goulon J, Finazzi M and Brookes N B 1998 Magnetocrystalline anisotropy in (111) $CoPt_3$ thin film with growth-induced chemical anisotropy investigated by x-ray magnetic circular dichroism *J. Appl. Phys.* **83** 6617

[8] Bruno P 1989 Tight-binding approach to the orbital magnetic moment and magnetocrystalline anisotropy of transition-metal monolayers *Phys. Rev.* B **39** 865

[9] van der Laan G 1998 Microscopic origin of magnetocrystalline anisotropy in transition metal thin films *J. Phys.: Condens. Matter* **10** 3239

[10] Ghiringhelli G, Bonfim M, Brookes N B, Camarero J, Mackay M, Montaigne F, Neisius T, Ohresser P, Pascarelli S, Petroff F, Pizzini S and Fontaine A 2001 *X-Ray Magnetic Circular Dichroism in the Investigation of Magnetic Dynamics in the Nanosecond Time Scale* (Berlin: Springer) p 347

[11] Duc F, Rikken G, Detlefs C and Sette F 2006 *Workshop on Synchrotron Applications of High Magnetic Fields (Grenoble)*

[12] Rogalev A, Wilhelm F, Jaouen N, Goulon J and Kappler J P 2003 *XAFS-12: Proc. 12th Int. Conf. on X-Ray Absorption Fine Structure (Malmö)*
[13] Yasui M and Shimizu M 1985 Relativistic formulae for the wavevector-dependent magnetic susceptibilities and the numerical calculation of the orbital and spin–orbit magnetic susceptibilities in vanadium *J. Phys. F: Met. Phys.* **15** 2365
[14] Deng M, Freyer H and Ebert H 2000 Spin and orbital magnetic susceptibility of the alloy system Ag_xPt_{1-x} *Solid State Commun.* **114** 365
[15] Deng M, Freyer H, Voitländer J and Ebert H 2001 Relativistic calculation of magnetic linear response functions using the Korringa–Kohn–Rostoker Green's function method *J. Phys.: Condens. Matter* **13** 8551
[16] Minár J and Ebert H 2004 Magnetic circular dichroism in x-ray absorption: theoretical description and applications *Appl. Phys.* A **78** 847
[17] Wohlfarth E P 1962 High magnetic field effects in ferromagnetic metals *Phys. Lett.* **3** 17
[18] Mankovsky S and Ebert H 2006 Theoretical description of the high-field susceptibility of magnetically ordered transition metal systems with applications to Fe, Co, Ni, and $Fe_{1-x}Co_x$ *Phys. Rev.* B **74** 54414
[19] Gunnarsson O 1976 Band model for magnetism of transition metals in the spin-density-functional formalism *J. Phys. F: Met. Phys.* **6** 587
[20] Janak J F 1977 Uniform susceptibilities of metallic elements *Phys. Rev.* B **16** 255
[21] Vosko S H and Perdew J P 1975 Theory of the spin susceptibility of an inhomogeneous electron gas via the density functional formalism *Can. J. Phys.* **53** 1385
[22] Durham P J 1984 *The Electronic Structure of Complex Systems* (New York: Plenum) p 709
[23] Ebert H 1996 Spin–orbit influenced spectroscopies of magnetic solids *Spin–Orbit Influenced Spectroscopies of Magnetic Solids* (*Springer Lecture Notes in Physics* vol 466) ed H Ebert and G Schütz (Berlin: Springer) p 159
[24] Schaich W L 1984 Derivation of single-scattering formulas for x-ray absorption and high-energy electron-loss spectroscopies *Phys. Rev.* B **29** 6513
[25] Ebert H 1996 Magneto-optical effects in transition metal systems *Rep. Prog. Phys.* **59** 1665
[26] Teramura Y, Tanaka A and Jo T 1996 Effect of Coulomb interaction on the x-ray magnetic circular dichroism spin sum rule in 3d transition elements *J. Phys. Soc. Japan* **65** 1053
[27] Park S Y, Muto S, Kimura A, Imada S, Kagoshima Y, Miyahara T, Hatano T, Hanyu T and Shiozaki I 1995 Magnetic circular dichroism of Ni–Pd alloys in Ni 2p, 3p, pd 3p, and 4p core excitation regions: enhancement of Ni 3d orbital moment *J. Phys. Soc. Japan* **64** 934
[28] Böske T, Clemens W, Carbone C and Eberhardt W 1994 Circular magnetic x-ray dichroism of 3d impurities in Ni *Phys. Rev.* B **49** 4003
[29] Ankudinov A and Rehr J J 1995 Calculation of x-ray magnetic circular dichroism in Gd *Phys. Rev.* B **52** 10214
[30] Benoist R, Carra P and Andersen O K 2000 Band structure and atomic sum rules for x-ray dichroism *Eur. J. Phys.* B **18** 193
[31] Wu R, Wang D and Freeman A J 1993 First principles investigation of the validity and range of applicability of the x-ray magnetic circular dichroism sum rule *Phys. Rev. Lett.* **71** 3581
[32] Guo G Y, Ebert H, Temmerman W M and Durham P J 1994 First principles calculation of magnetic x-ray dichroism in Fe and Co multilayers *Phys. Rev.* B **50** 3861
[33] Guo G Y, Ebert H, Temmerman W M and Durham P J 1995 Band theoretical investigation of circular magnetic x-ray dichroism in Fe and Co multilayers *J. Magn. Magn. Mater.* **148** 66
[34] Wu R, Wang D and Freeman A J 1994 Validity and the applicability of magnetic-circular-dichroism sum rules for transition metals *J. Appl. Phys.* **75** 5802
[35] Wu R Q and Freeman A J 1994 Limitation of the magnetic-circular-dichroism spin sum-rule for transition-metals and importance of the magnetic dipole term *Phys. Rev. Lett.* **73** 1994
[36] Wu R, Wang D and Freeman A J 1994 First principles investigations of MCD spectra and sum rules for 3d transition metal surfaces *J. Magn. Magn. Mater.* **132** 103
[37] Strange P 1994 Magnetic absorption dichroism and sum-rules in itinerant magnets *J. Phys.: Condens. Matter* **6** L491
[38] Mankovsky S and Ebert H 2004 Theoretical description of field-induced magnetic circular x-ray dichroism in nonmagnetic solids *Phys. Rev.* B **69** 14414
[39] Ebert H and Mankovskyy S 2003 Field-induced magnetic circular x-ray dichroism in paramagnetic solids: a new magneto-optical effect *Phys. Rev. Lett.* **90** 077404
[40] Ebert H 2000 Fully relativistic band structure calculations for magnetic solids—formalism and application *Electronic Structure and Physical Properties of Solids* (*Springer Lecture Notes in Physics* vol 535) ed H Dreyssé (Berlin: Springer) p 191